Mineralogical Characterization and Preliminary Beneficiation of the Zoro Lithium Project, Manitoba, Canada

Tassos Grammatikopoulos[1] · Massoud Aghamirian[1] · Mark Fedikow[2] · Toby Mayo[3]

Abstract

The Zoro pegmatite project in east-central Manitoba occurs 20 km east of the historic mining town of Snow Lake. A composite sample (Master Comp) was prepared from three pegmatite zones within Zoro Dyke "D1" including the North, Central, and South Zones for mineralogical analysis and heavy liquid separation (HLS). The mineralogical examination was conducted on a subsample crushed to ca. P_{80} of 600 μm to determine the overall mineral assemblage, liberation of spodumene, and assess the potential recovery of spodumene by flotation. XRD and QEMSCAN results show that the sample consists of spodumene (10.5%), quartz (29.3%), plagioclase (29.0%), K-feldspars (21.3%), micas (5.1%), tourmaline (2.9%), and Fe-Mn-phosphates (0.1%). Spodumene is well liberated (88%), but also forms complex particles (7%), and middlings with quartz (4%). Liberation of spodumene increases from 81 in the + 600 μm to 95% in the − 106 μm size fraction. Liberation of quartz, feldspars, and micas account for 89%, 94%, and 83%, respectively. Electron probe micro-analyses and LA-ICP-MS showed that the average Li concentration is 3.7% in spodumene, 2196 ppm in micas, 1001 ppm in tourmaline, and 115 ppm in K-feldspars. Thus, spodumene accounts for 96%, micas 2%, Fe-Mn phosphates 1%, and both K-feldspars and tourmaline for < 1% of the total Li in the sample. The mineralogical data indicate the potential to recover spodumene by flotation with minimal Li losses due to other than spodumene carriers. Heavy liquid separation was conducted on the Master Comp which was crushed to − 6.4 mm, while the − 600 μm fraction was removed from this test. The coarse fraction − 6.4 mm/+ 600 μm was subjected to HLS tests with eight heavy liquid-specific gravity cut-points (2.65 to 3.10 g/cm³). HLS indicates that it is possible to produce a high-grade lithium concentrate (close to 6% Li_2O) after the rejection of iron silicates with magnetic separation.

Keywords Zoro pegmatite · Spodumene pegmatites · Li · QEMSCAN characterization · Heavy liquid separation

1 Introduction

Lithium is a soft, silver-white alkali metal with atomic number 3. The end use of lithium was estimated to be for lithium-ion batteries (35%), ceramics and glass (32%), lubricating greases (9%), air treatment (5%), continuous casting mold flux powders (5%), polymer production (4%), primary aluminum production (1%), and other uses (9%) [1].

Lithium is found in brine lake deposits containing lithium chloride and in hard rock pegmatite deposits. It can be sold in a range of product types, as mineral concentrate, brine, compound (lithium carbonate or lithium hydroxide), and metal depending on its intended end use [1, 2]. Lithium occurs in a large number of minerals such as spodumene ($LiAlSi_2O_6$), amblygonite, $(Li,Na)Al(PO_4)(F,OH)$, zinnwaldite, $KLiFeAl(AlSi_3)O_{10}(F,OH)_2$, petalite ($LiAlSi_4O_{10}$), and lepidolite $K(Li,Al)_3(Si,Al)_4O_{10}(F,OH)_2$ [3]. However, spodumene is the most prevalent economic lithium-bearing mineral [4]. It is an alumino-silicate mineral with the chemical formula $Li_4Al_4[SiO_3]_8$, composed of silica tetrahedral bound laterally through ionic bonding with lithium and aluminum in octahedral co-ordinations [5]. It is tabular and insoluble in acids [3].

Spodumene occurs in pegmatite deposits along with other silicate minerals such as feldspars, micas, and quartz (e.g., [6] and references therein). There are three types of spodumene that can occur including phenocrystic spodumene in un-zoned pegmatite with a Fe_2O_3 content of 0.6–0.9% (Fe substitutes

✉ Tassos Grammatikopoulos
  Tassos.Grammatikopoulos@sgs.com

1 SGS Canada Inc., Lakefield, On K0L 2H0, Canada

2 Mount Morgan Resources Ltd., Salt Spring Island, British Columbia V8K 1E3, Canada

3 Far Resources Ltd., 550 - 800 West Pender Street, Vancouver, BC V6C 2V6, Canada

for Al in the spodumene crystal structure), zonal spodumene with a Fe_2O_3 content of 0.01–0.03%, and spodumene plus quartz aggregates pseudomorphs after petalite with and Fe_2O_3 content of 0.007–0.03%. Primarily, the phenocrystic spodumene is found in deposits that can be economically mined [7]. Spodumene-bearing pegmatite deposits range in lithium head grades from 1% Li_2O in low-grade deposits to 4% L_2O in higher grade deposits [8].

The mineralogy of hard rock Li deposits is not always well understood in exploration. Exploration and mining companies rely heavily on geochemistry to delineate the reserves. Conventional techniques such as X-ray diffraction (XRD) can provide guidance to the main Li phases (e.g., spodumene, petalite) assuming detectable amounts (> 1–2%) are present. However, other Li-bearing minerals such as phosphates, micas, and tourmaline can contain significant Li concentrations and may not be identified with the XRD properly if they occur in low-grade samples. For example, XRD can identify lepidolite group micas, but also muscovite micas which can host considerable Li, and therefore, the results can be misleading. Micas form solid solution series and do not have a fixed Li concentration. Furthermore, geochemical analyses cannot be properly used to determine the Li minerals even when the bulk mineralogy is known due to the presence of a number of Li minerals in the deposits. Automated mineralogy can be used to improve the understating of the mineralogical characteristics, identify low-grade Li-bearing minerals, and determine the liberation of the main and subordinate Li phases, and gangue minerals. However, SEM-based instruments cannot detect Li. Therefore, it is critical that automated mineralogy is coupled with XRD and mineral chemistry. Electron probe micro-analyses (EPMA) are useful to determine the major elements of the various minerals, e.g., FeO in spodumene since it will affect its final end use. Laser ablation by inductively coupled plasma mass spectrometry (LA-ICP-MS) is used to determine not only the concentration of Li but other low-grade elements such as Ga, Cs, and Rb in spodumene, petalite, micas, phosphates, and other minerals. The data are then coupled to calculate the Li distribution and evaluate the mineralogy of the deposit.

Spodumene is the most common and abundant lithium mineral with the highest concentration of lithium. Proper mineralogical characterization of the spodumene characteristics can impact the lithium production. Automated mineralogy has been used to quantify mineralogical attributes of various projects including lithium minerals (e.g., [9, 10]). This paper focuses on (i) the mineralogical characteristics of a finely ground sample to evaluate mineralogical parameters, i.e., type of Li minerals, grades, and their liberation to assist flotation, and (ii) preliminary beneficiation of a coarsely ground sample using heavy liquid separation (HLS) to upgrade spodumene for the production of a concentrate suitable for lithium extraction by hydrometallurgical operations.

2 Location and Geology of the Zoro Lithium Project

The Zoro Lithium Project is located in east-central Manitoba, 20 km east of the historic mining town of Snow Lake (Fig. 1). The property consists of 16 claims with a total of 3603 ha and is proximal to excellent infrastructure. Exploration has been rapidly advanced on the property with an integrated program of prospecting, innovative soil geochemical surveys, and five diamond drill programs totaling 8406 m in 60 holes.

Abundant overburden cover characterizes much of the property, and the pegmatite dykes do not have a consistent recognizable geophysical signature. Light green to white spodumene mineralization occurs within laterally and vertically extensive pegmatite dykes hosted by a variety of lithologies. There are no preferred host rocks for the dykes. The spodumene-bearing pegmatite dykes on the property strike northwest with steep dips and crosscut the regional foliation at a low angle. They are up to 800 m in length and 40 m in drill intersection. The dykes tend to be concentric in internal structure and constituent minerals include potassium feldspar, quartz, spodumene, and black tourmaline. A maiden resource of 1.1Mt at 0.91% Li_2O was reported on a portion of dyke D1 in 2018.

Five successful drill campaigns have been completed on the property, leading to the discovery of 13 lithium-bearing pegmatite dykes, as the company advances their understanding of a major dyke swarm on the 30 km^2 Zoro property. The 36.5-m-wide D8 dyke was discovered by diamond drill testing a Mobile Metal Ions' (MMI) soil geochemical anomaly. D8 has a strike length of at least 90 m with down dip intersections of 100 m and true thickness of up to 15 m and is open in all directions. Five additional dykes were discovered during the 2018/2019 winter drill campaign drilling MMI anomalies thereby confirming the usefulness of this technique for exploration beneath cover on the property. Exploration proceeds on the Zoro property with more than fifty additional untested geological and MMI geochemical targets.

3 Methodology

3.1 Sample Preparation

Samples of sawn core from Zoro Pegmatite D1, referred to as Zoro North, Central, and South Zones, and adjacent host rocks (quartz porphyry and amphibolite) were investigated. Each pegmatite sample was stage-crushed to 1 in. Subsamples were riffled and pulverized for chemical assays for major elements and lithium. The three pegmatite samples were properly blended to generate a composite (Master Comp) that was used for mineralogical examination and heavy liquid separation

Fig. 1 Location map and local geology showing the spodumene pegmatites
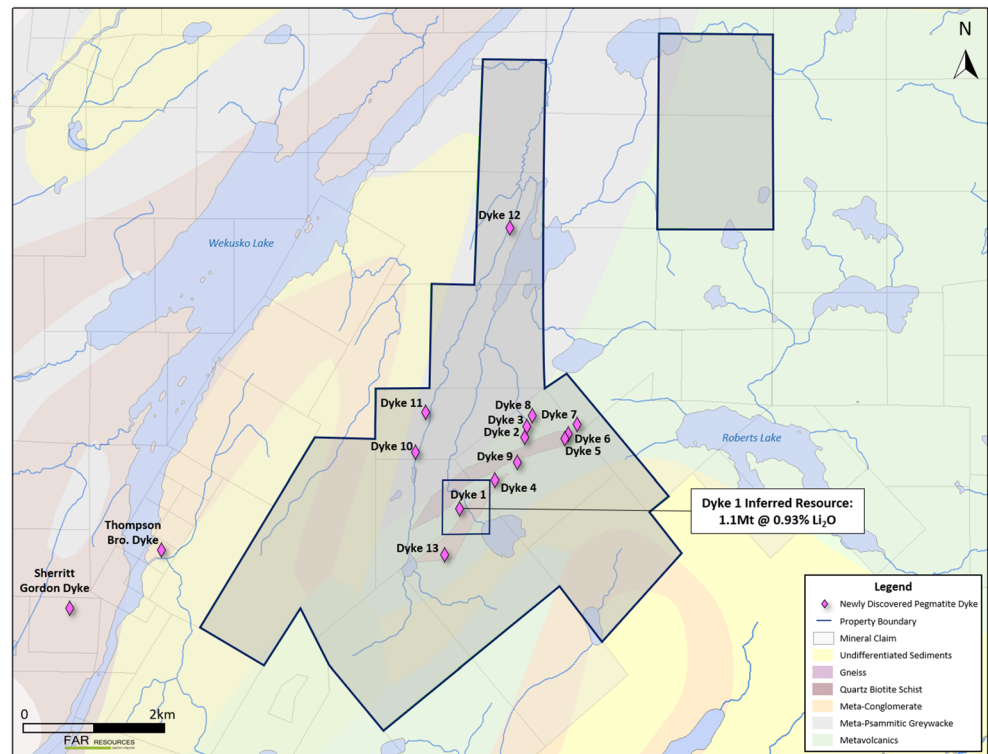
(HLS) testwork. The mineralogical attributes of the host rocks were also investigated but not reported in this paper.

An approximate 0.85-kg subsample for mineralogical examination was stage-crushed to ca. of P_{80} of 600 μm. A micro-riffled subsample was submitted for X-ray diffraction analysis. Approximately, 500 g were screened and combined into four size fractions including + 600 μm, − 600/+ 300 μm, − 300/+ 106 μm, and − 106 μm for the mineralogical work. Graphite-impregnated polished epoxy grain mounts were prepared from the different fractions. A subsample was micro-riffled from each size fraction for whole rock analysis for major elements and tantalum by X-ray fluorescence (XRF). Cesium and rubidium were analyzed by ICP-MS, and lithium by AAS subsequent to a sodium peroxide fusion. Analyses were conducted at SGS Canada Inc., Lakefield site, ON.

Furthermore, the Master Comp sample was stage-crushed to − 6.4 mm for the HLS testwork. Following crushing, the sample was first screened to remove the – 600-μm fraction, which is considered the cut-off particle size for effective dense media separation. The − 6.4 mm/+ 600 μm was then submitted for separate HLS tests, each of which included eight heavy liquid-specific gravity cut-points (3.10, 3.00, 2.95, 2.90, 2.80, 2.70, 2.65).

3.2 Mineral Chemistry

Electron probe micro-analyses (EPMA) were conducted with a JEOL JXA-733 EPMA operating at 15 kV and 30 nA. The microprobe is equipped with dSspec and dQant32 automation (Geller MicroAnalytical). The minerals were analyzed with the electron microprobe, marked, and their coordinates were transferred to the LA-ICP-MS. The laser ablation inductively coupled plasma mass spectrometry (LA-ICP-MS) was conducted at the University of New Brunswick, Fredericton, NB, Canada. The Department of Earth Sciences houses a Resonetics S-155-LR 193-nm Excimer laser ablation system coupled to an Agilent 7700x quadrupole ICP-MS. The S-155 cell, designed by Laurin Technic Pty, is a two-volume small volume ablation cell that provides unmatched signal washout and stability. Note that the minerals analyzed with the electron microprobe were marked and their coordinates were transferred to the LA-ICP-MS. Two- to three-point analyses were conducted for each electron microprobe analysis to avoid micrometric inclusions of other minerals and adjacent minerals.

3.3 QEMSCAN Operational Modes and Quality Control

QEMSCAN analysis was conducted at the Advanced Mineralogy Facility at SGS Canada, Lakefield site. QEMSCAN is an EVO 430 automated scanning electron microscope, which is equipped with four light element energy dispersive X-ray spectrometers and iDiscover software capable of processing the data and images. QEMSCAN operates with a 25-kV accelerating voltage and a 5-nA beam current. The QEMSCAN measures and the iDiscover software

Table 1 Geochemical results including major elements and Li of the different pegmatite samples

Sample ID	Zoro North Pegmatite	Zoro Central Pegmatite	Zoro South Pegmatite	Master Comp
Li%	0.34	0.39	0.54	0.44
SiO2%	70.60	72.10	71.70	71.90
Al2O3%	15.90	15.90	16.20	15.90
Fe2O3%	1.19	0.97	1.25	1.06
MgO%	0.31	0.08	0.22	0.20
CaO%	0.63	0.39	0.62	0.51
Na2O%	3.23	3.50	3.76	3.48
K2O%	4.35	4.31	3.12	3.91
TiO2%	0.02	0.02	0.02	0.02
P2O5%	0.26	0.27	0.21	0.22
MnO%	0.03	0.04	0.03	0.04
Cr2O3%	0.02	< 0.01	0.01	< 0.01
V2O5%	< 0.01	< 0.01	< 0.01	< 0.01
LOI%	1.64	1.19	1.41	1.27
Sum%	98.20	98.80	98.60	98.60

processes data from every pixel across a sample with a measurement resolution defined based on the scope of the analysis. The software assigns each pixel a mineral name based on 1000 counts of energy dispersive X-ray spectral data and backscatter electron intensities. If the minerals or constituent phases comprising the sample are compositionally distinct, QEMSCAN is capable of reliably discriminating and

quantifying them. The mode of the QEMSCAN analysis used for this project was the particle mineral analysis (PMA). A predefined number of particles were mapped at a point of 3 to 8-μm pixel size to spatially resolve and describe mineral grain textures and associations. The PMA mode scans the polished section and provides a statistically robust population of mineral identifications based on the X-ray chemistry of minerals. Light elements such as lithium, boron, carbon, beryllium, oxygen, and hydrogen cannot be discriminated by the QEMSCAN analysis. Thus, the identification of spodumene was based on the aluminum-silica ratios.

The liberation and association characteristics of spodumene are determined by size fraction and calculated for the head. For the purposes of this analysis, particle liberation is defined based on 2D particle area percent. Particles are classified in the following groups (in descending order) based on mineral-of-interest area percent: free ($\geq 95\%$ of the total particle area) and liberated ($\geq 80\%$). The non-liberated grains have been classified according to association characteristics, where binary association groups refer to particle area percent

Table 2 Geochemical results including major elements and Li from the various size fractions of the Master Comp

Sample ID	+ 600 μm	− 600/ + 300 μm	− 300/ + 106 μm	− 106 μm
Li%	0.54	0.39	0.36	0.31
SiO2%	72.30	74.20	72.50	69.60
Al2O3%	16.30	15.00	15.20	16.50
Fe2O3%	0.96	0.97	1.15	1.30
MgO%	0.19	0.18	0.19	0.32
CaO%	0.42	0.43	0.51	0.85
Na2O%	3.23	3.37	3.47	3.71
K2O%	3.88	3.68	3.76	4.19
TiO2%	0.02	0.02	0.02	0.03
P2O5%	0.19	0.22	0.24	0.32
MnO%	0.03	0.02	0.03	0.03
Cr2O3%	0.01	0.02	0.02	0.02
V2O5%	< 0.01	< 0.01	< 0.01	< 0.01
LOI%	1.00	0.92	0.96	1.35
Sum%	98.5	99	98.1	98.2
Cs (ppm)	243	246	268	268
Ta (ppm)	37	34	56	80
Rb (ppm)	1530	1490	1500	1640

Table 3 Lithium assays, weight distribution, and lithium distribution (Dist.) by size fraction of the Master Comp

Fraction	Chemical Li%	wt% Dist.	Li% Dist.
Combined	0.40*	100	100
+ 600 μm	0.54	27.4	36.5
600/+ 300 μm	0.39	24.4	23.5
300/+ 106 μm	0.36	24.6	21.9
− 106 μm	0.31	23.6	18.1

* Calculated

Fig. 2 Mass wt% and Li% distribution by size fraction if the Master Comp
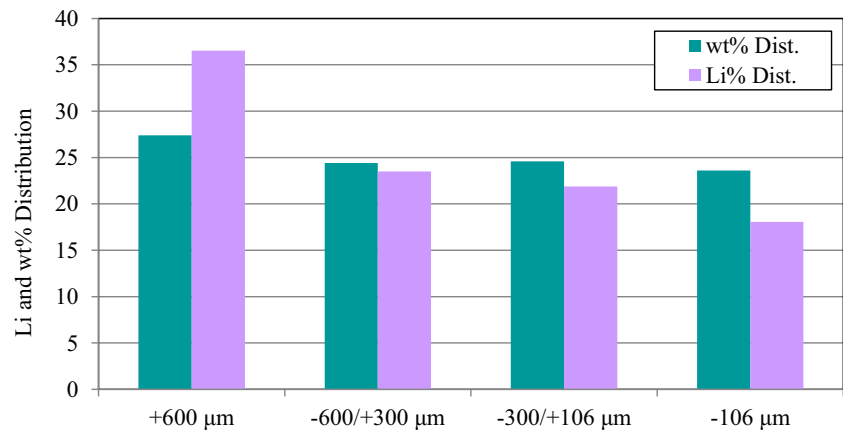
greater than or equal to 95% of the two minerals or mineral groups. The complex groups refer to particles with ternary, quaternary, and greater mineral associations including the mineral of interest.

4 Results

4.1 Geochemistry

Lithium grades are similar in the North and Central Pegmatite at 0.34% and 0.39%, respectively, but significantly higher in the South Pegmatite (0.54%) (Table 1). The lithium concentration in the Master Comp is 0.44%. The Li grades indicate potential zoning or variability within the dyke complex which has to be further explored for possible geochemical trends. The Li grades can affect the final concentrate grades depending on the blending proportions of the three samples. The results from the Master Comp reflect a blend of equal proportions of each sample used.

Table 4 Chemical (Chem) assays vs. calculated assays from the QEMSCAN (QS) for the head sample

Element (wt%)	QS	Chem
Al	8.13	8.34
Ca	0.43	0.39
Fe	0.74	0.76
K	3.13	3.22
Li	0.39	0.40
Mg	0.10	0.13
Na	2.47	2.55
P	0.10	0.10
Rb	0.15	0.15
Si	34.0	33.7

4.2 Mineralogical Results

4.2.1 Geochemistry by Size Fraction, Mass Balance, and Lithium Distribution

The size by size assays of the Master Comp including the major elements, lithium, tantalum, cesium, and rubidium is shown in Table 2. Lithium concentration is highest in the + 600 μm at 0.54% and decreases in the finer fractions to 0.39%, 0.36%, and 0.31 wt%. Tantalum grades range from 34 to < 80 ppm, cesium from 243 to 268 ppm, and rubidium from 1490 to 1640 ppm. The mass distribution (wt%) is approximately similar in the size fractions (Table 3, Fig. 2). However, the + 600-μm size fraction accounts for most of the Li (36.5%) in the sample which gradually decreases with decreasing size (23.5%, 21.9%, and 18.1%). This indicates that spodumene remained relatively coarse during crushing and grinding.

4.2.2 QEMSCAN Assay Reconciliation

The chemical assays in Table 4 are used as quality control to ensure that there were no analytical flaws during the QEMSCAN analysis. The QEMSCAN assays are calculated based on mass of each mineral and wt% and are compared against the calculated chemical assays from each size fraction as a function of their wt%. It is critical to note that the chemistry of the minerals is adjusted in the iDiscover software based on the EPMA and LA-ICP-MS analyses. Reconciliation is considered very good.
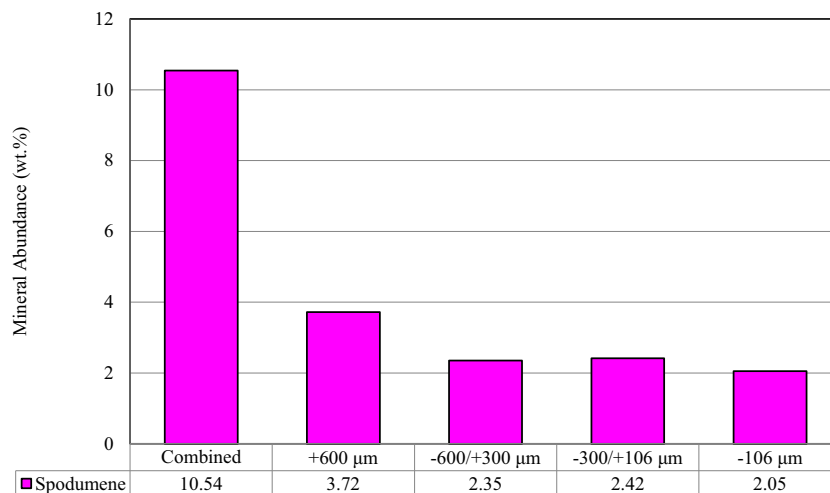
4.2.3 Mineral Abundance

X-ray diffraction analysis was conducted to verify the bulk mineral assemblage and the main lithium minerals. XRD identified mainly plagioclase and quartz, moderate K-feldspars, spodumene, and minor mica. The mineral abundances (in wt%) were determined with the QEMSCAN, and the results

Table 5 Modal abundance (wt%) by size fraction and calculated for the head for the Master Comp

Mineral/fraction	Combined	+ 600 μm	− 600/ + 300 μm	− 300/ + 106 μm	− 106 μm
Spodumene	10.5	13.6	9.61	9.84	8.72
Quartz	29.3	29.3	34.1	29.8	23.9
Plagioclase	29.0	28.1	27.9	29.4	30.9
K-Feldspar	21.3	21.1	19.9	20.5	23.8
Muscovite	4.34	3.61	3.40	4.61	5.89
Biotite	0.75	0.95	0.50	0.91	0.60
Apatite	0.50	0.62	0.46	0.46	0.45
Tourmaline	2.91	1.76	2.67	3.33	4.07
Sulfides	0.19	0.13	0.29	0.15	0.20
Fe-(Ti)-(Mn)-Oxides	0.06	0.01	0.02	0.02	0.19
Nb-Ta-Ox	0.01	0.01	0.01	0.01	0.01
Amphibole	0.59	0.60	0.80	0.45	0.51
Titanite	0.02	0.01	0.02	0.00	0.04
Carbonates	0.34	0.21	0.20	0.32	0.64
Li-phosphates	0.10	0.01	0.15	0.10	0.14
Other	0.00	0.00	0.01	0.00	0.01
Total	100	100	100	100	100

are shown by size fraction and calculated head (Table 5). The analysis by size is conducted to determine possible preferred accumulation of any mineral in any one size fraction and better estimate the liberation of the minerals. QEMSCAN analysis of the calculated head yields spodumene (10.5%), quartz (29.3%), plagioclase (29.0%), K-feldspars (21.3%), micas (5.1%), and traces of Li-bearing phosphates (0.1%), tourmaline, and other minerals. The coarse fraction, + 600 μm, accounts for 3.7% of the total mass of spodumene (10.5%), while the spodumene ranges from 2.1 to 2.4% in the finer fractions (Fig. 3). Other minerals show also minor variations in the size fractions.

4.2.4 Grain Size Distribution

The cumulative grain size distribution of spodumene, quartz, feldspars, micas, and overall particle size of the sample is illustrated in Fig. 4. Quartz is the coarsest mineral with a D_{50} of 247 μm, followed by spodumene at 205 μm and feldspars at 184 μm, while micas are the finest at 81 μm. The term particle refers to both liberated and middling particles, monomineralic, and polymineralic and has a D_{50} of 216 μm (D_{80} is 505 μm and D_{100} is 733 μm).

The particle size and distribution of spodumene and gangue minerals are critical for flotation purposes. It is well known

Fig. 3 Distribution (absolute mass) of spodumene by size fraction and calculated head

	Combined	+600 μm	-600/+300 μm	-300/+106 μm	-106 μm
Spodumene	10.54	3.72	2.35	2.42	2.05

Fig. 4 Cumulative grain size distribution for the head sample
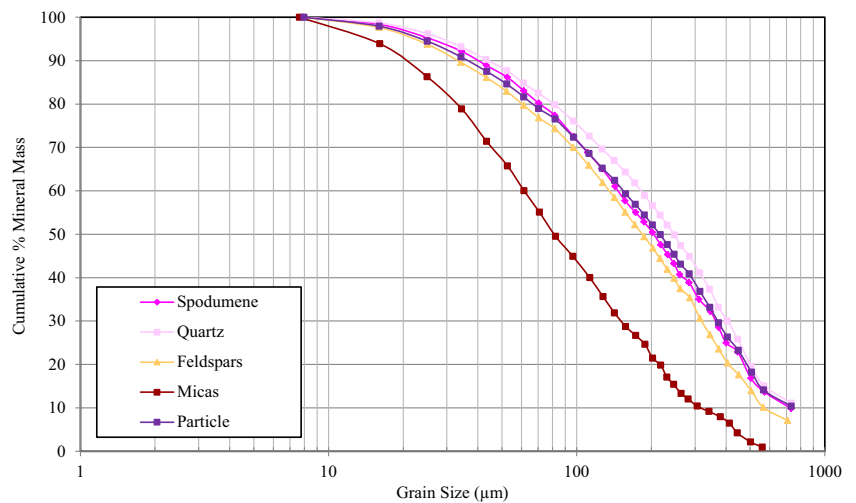
that as the mineral particle size is gradually reduced during processing, the mineral's shape and surface properties become more important [11, 12]. Particle size might also affect surface chemistry of spodumene. For example, Xu et al. [13] evaluated the flotation and adsorption of sodium oleate (NaOL) on spodumene with four different particle size fractions (45–75 μm, 38–45 μm, 19–38 μm, and 0–19 μm). The flotation recovery increases upon slightly decreasing the size fraction, reaching a peak value at a size fraction of 38–45 μm, but recovery decreases in the fine grain sizes. They attributed this trend the Al-O bonds of the spodumene and changes in its surface crystal chemistry. The {110} plane of spodumene is more favorable for chemisorbing NaOL than the {001} plane, which has one broken Al-O bond. Filippov et al. [14] came to similar conclusions. They note that the {110} plane is the weakest plane, and spodumene has the highest tendency to cleave along this plane. Therefore, selective grinding might increase the amounts of spodumene with {110} planes to increase its recovery. It is possible that spodumene might

behave differently during flotation at even coarser grain sizes, but this would have to be validated with flotation experiments.

The normalized mass distribution of spodumene as a function of its aspect ratio (AR) by size fraction and size class are illustrated in Figs. 5 and 6, respectively.

Selected spodumene particles with aspect ratio of > 3:< 4 and > 2:< 2.5 are depicted in Fig. 7. Most of the spodumene has an aspect ratio between 1 and 2. The aspect ratio could be used as a guide to assess the {110} planes of spodumene; the higher the aspect ratio should reflect a higher abundance of {110} spodumene planes. Spodumene is generally coarse-grained in the current testwork. However, selective grinding along the long axis of the spodumene will increase its aspect ratio and thus the {110} planes.

4.2.5 Liberation and Association of Spodumene and Gangue Minerals

Liberation (free and liberated collectively) of spodumene in the sample is very good at 88% (Fig. 8) for the target grind size of a P_{80} of 600 μm. The non-liberated spodumene occurs as complex particles (6.8%) and middlings with quartz (3.7%). Liberation of spodumene increases from 81 in the + 600 μm to 95% in the – 106-μm size fraction (Fig. 8). Free spodumene (most pure) increases from 73 to 90%, while liberated decreases from 8 to 5% from the coarsest to the finest fraction. Therefore, finer grinding will increase the liberation, i.e., purity of the mineral.

The particle liberation by size (Fig. 9), calculated for the head sample, indicates that free and liberated particles and middling particles occur at different proportions in size classes from 25 to 800 μm. The occurrence of spodumene suggests that a rougher flotation concentrate with high recovery could be considered, followed by finer grinding to further liberate
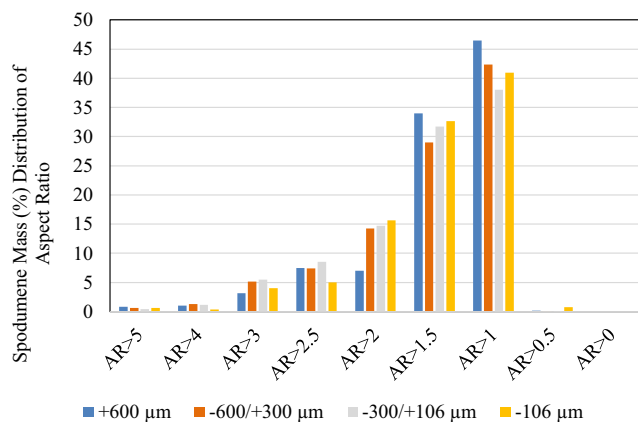

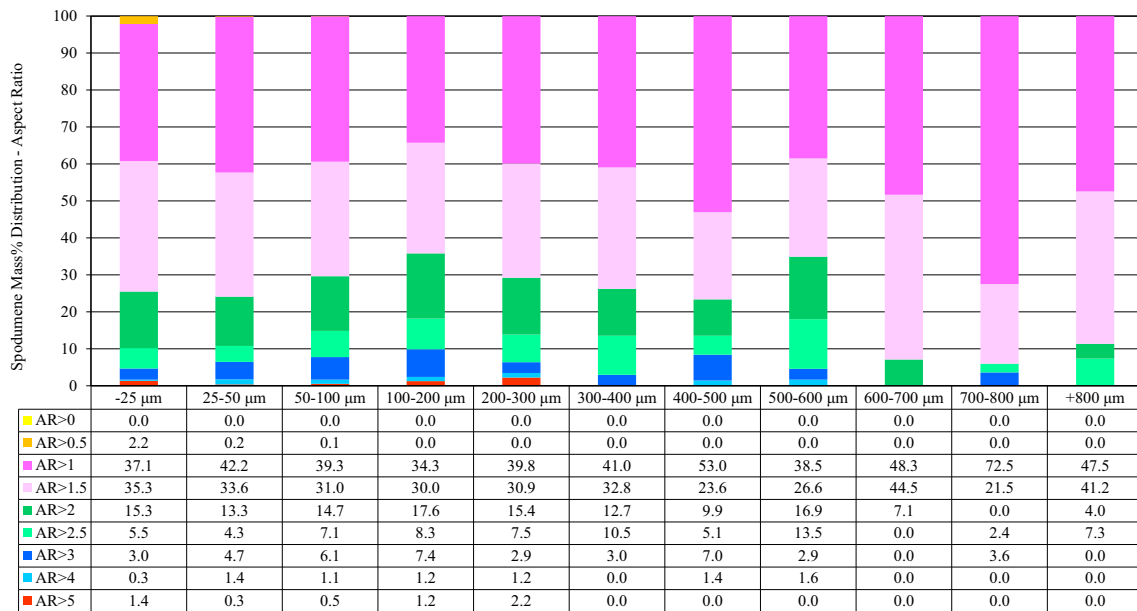Fig. 5 Aspect ratio (AR) of spodumene by size fraction

	-25 µm	25-50 µm	50-100 µm	100-200 µm	200-300 µm	300-400 µm	400-500 µm	500-600 µm	600-700 µm	700-800 µm	+800 µm
AR>0	0.0	0.0	0.0	0.0	0.0	0.0	0.0	0.0	0.0	0.0	0.0
AR>0.5	2.2	0.2	0.1	0.0	0.0	0.0	0.0	0.0	0.0	0.0	0.0
AR>1	37.1	42.2	39.3	34.3	39.8	41.0	53.0	38.5	48.3	72.5	47.5
AR>1.5	35.3	33.6	31.0	30.0	30.9	32.8	23.6	26.6	44.5	21.5	41.2
AR>2	15.3	13.3	14.7	17.6	15.4	12.7	9.9	16.9	7.1	0.0	4.0
AR>2.5	5.5	4.3	7.1	8.3	7.5	10.5	5.1	13.5	0.0	2.4	7.3
AR>3	3.0	4.7	6.1	7.4	2.9	3.0	7.0	2.9	0.0	3.6	0.0
AR>4	0.3	1.4	1.1	1.2	1.2	0.0	1.4	1.6	0.0	0.0	0.0
AR>5	1.4	0.3	0.5	1.2	2.2	0.0	0.0	0.0	0.0	0.0	0.0

Fig. 6 Aspect ratio of spodumene by conventional size class

the spodumene at a cleaner stage during flotation. However, the additional liberation of the spodumene is a function of the grinding cost and a desire grade and recovery.

The nature of the association of spodumene with the gangue minerals is critical to understand potential impurities in the final concentrate. The textural variations of spodumene with gangue minerals varies (Fig. 10). Free spodumene occurs as prismatic, tabular, and stubby habits. It also forms simple middlings with slightly crenulated and straight grain contacts which are expected to liberate from each other upon additional grinding. However, it also forms complexly intergrown middlings with gangue minerals, hosts, or occurs as fine-grained inclusions in gangue, and contacts are crenulated with deep interpenetration. Therefore, some middling particles will still occur and, if recovered, will be reported in the final concentrate. Such characteristics reflect the geological aspects of the rocks. They are common in several spodumene pegmatites around the world (e.g., [10, 15, 16]). In particular, spodumene-quartz intergrowths (SQI) is a common texture in Li pegmatites [17] and have been interpreted as isochemical breakdown of petalite [18, 19]. Although automated mineralogy does not aim to resolve petrological aspects of the rocks, it can quantify such associations of spodumene with gangue minerals to evaluate the spodumene during processing. The mineralogical characteristics of the ore will dictate the final purity of the concentrate.

The exposed surface of the spodumene (Fig. 11) illustrates that 99% is well exposed (> 30% exposure). Exposure is similar to the liberation, but it is defined as the surface area percentage of the spodumene exposed within a composite particle. This parameter is employed to identify and classify particles according to their floatability. In contrast, the liberation does not define the exposed surface area of the spodumene, except for well-liberated grains. Empirically, spodumene particles with less than 20–30% exposure will likely not be recovered. Therefore, the potential to recover most of the spodumene favors flotation.

The liberation (Fig. 12) of each gangue mineral, especially by size fraction, is critical because minerals may respond differently during flotation. Liberation of quartz (89%), feldspars (94%), and micas (82%) is considered very good for this grind size. This indicates that the gangue minerals could be rejected
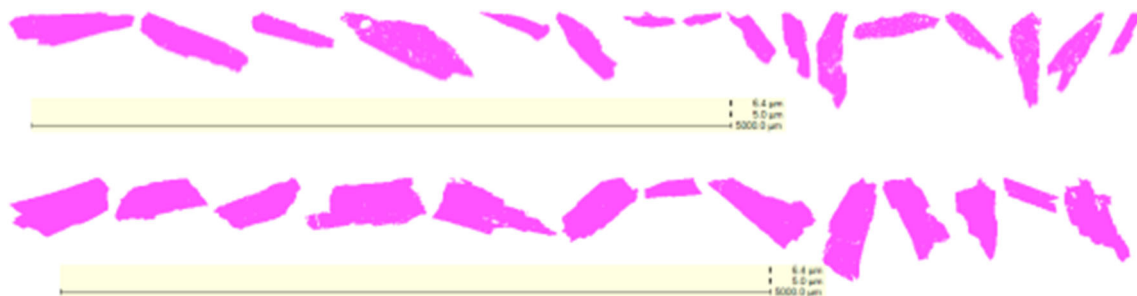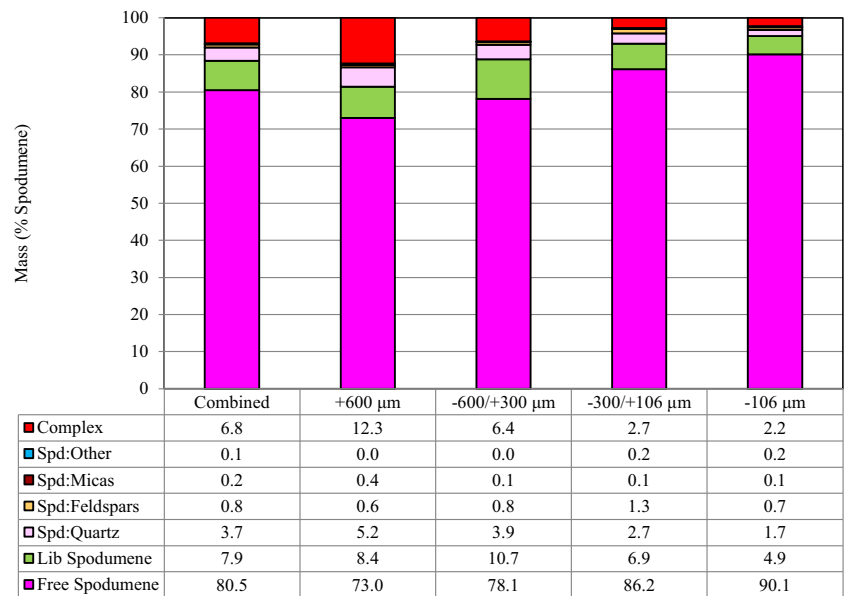

Fig. 7 Particle maps illustrating spodumene with AR > 3:< 4 (above) and AR > 2:< 2.5 (below) from the + 300 µm size fraction

Fig. 8 Spodumene liberation and association profile by size fraction and calculated for the head

	Combined	+600 μm	-600/+300 μm	-300/+106 μm	-106 μm
■ Complex	6.8	12.3	6.4	2.7	2.2
■ Spd:Other	0.1	0.0	0.0	0.2	0.2
■ Spd:Micas	0.2	0.4	0.1	0.1	0.1
□ Spd:Feldspars	0.8	0.6	0.8	1.3	0.7
□ Spd:Quartz	3.7	5.2	3.9	2.7	1.7
■ Lib Spodumene	7.9	8.4	10.7	6.9	4.9
■ Free Spodumene	80.5	73.0	78.1	86.2	90.1

during flotation to produce a high-grade Li concentrate. Furthermore, K-feldspars and micas could be further separated as by-products. Separation of such silicates is not always an easy process [3]. Tian et al. [20] investigated the flotation performance of spodumene and feldspars with four size ranges (0–19 μm, 19–38 μm, 38–45 μm, and 45–75 μm) in a single mineral micro-flotation test. Their results showed that

the maximum spodumene recovery is obtained with coarse particles of 38–45 μm, while for feldspar, the best flotation performance is found with fine particles of 0–19 μm. However, it is not clear how the gangue minerals might respond at coarser sizes. Thus, experimental flotation work of the gangue minerals at coarser sizes such as investigated by Tian et al. might help to understand their response.

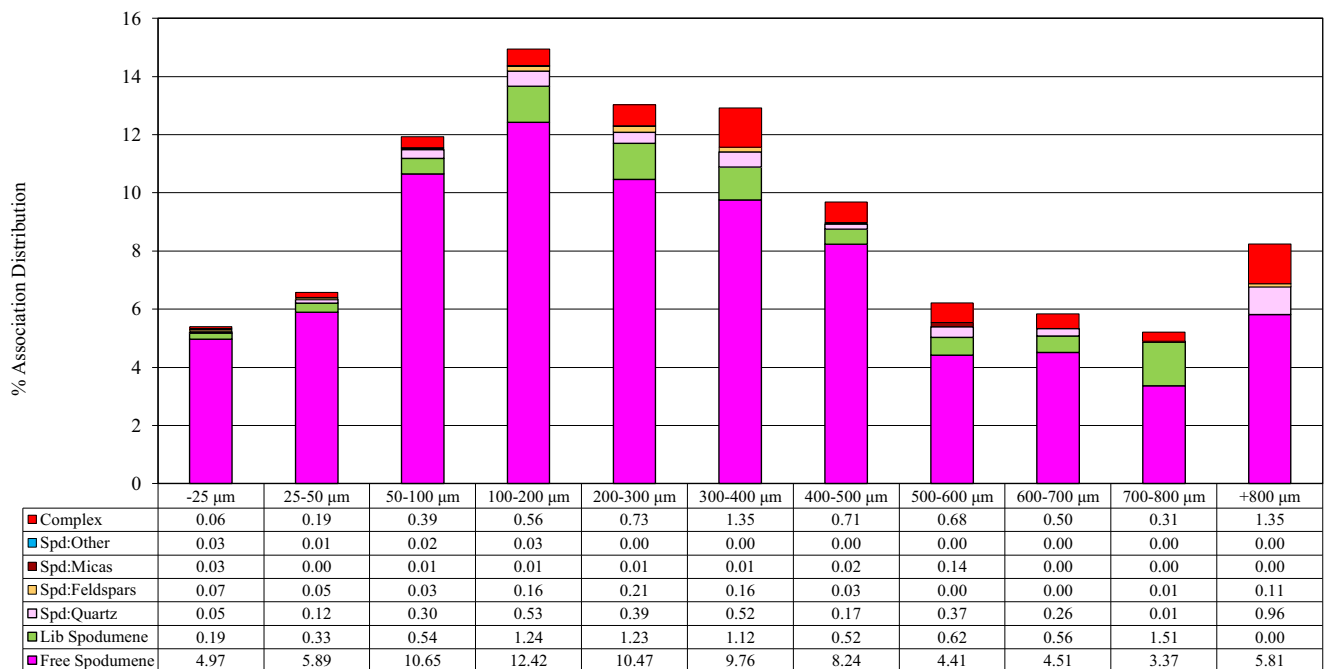|	-25 μm	25-50 μm	50-100 μm	100-200 μm	200-300 μm	300-400 μm	400-500 μm	500-600 μm	600-700 μm	700-800 μm	+800 μm
■ Complex	0.06	0.19	0.39	0.56	0.73	1.35	0.71	0.68	0.50	0.31	1.35
■ Spd:Other	0.03	0.01	0.02	0.03	0.00	0.00	0.00	0.00	0.00	0.00	0.00
■ Spd:Micas	0.03	0.00	0.01	0.01	0.01	0.01	0.02	0.14	0.00	0.00	0.00
□ Spd:Feldspars	0.07	0.05	0.03	0.16	0.21	0.16	0.03	0.00	0.00	0.01	0.11
□ Spd:Quartz	0.05	0.12	0.30	0.53	0.39	0.52	0.17	0.37	0.26	0.01	0.96
■ Lib Spodumene	0.19	0.33	0.54	1.24	1.23	1.12	0.52	0.62	0.56	1.51	0.00
■ Free Spodumene	4.97	5.89	10.65	12.42	10.47	9.76	8.24	4.41	4.51	3.37	5.81

Fig. 9 Spodumene liberation and association by conventionally made up size classes calculated for the head sample
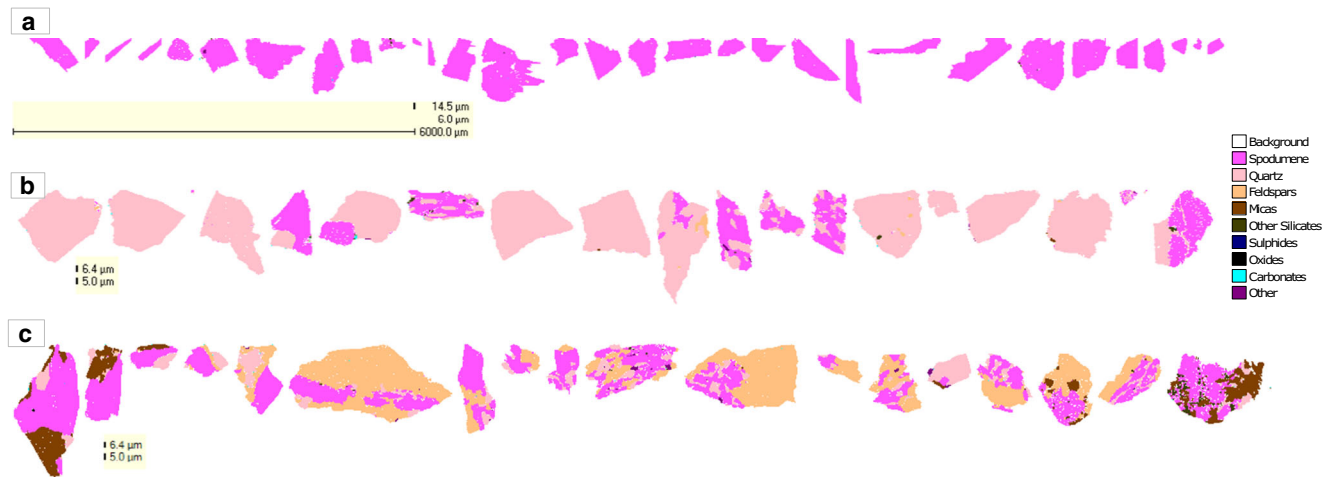
Fig. 10 Particle maps of (**a**) free spodumene from the + 600 μm fraction, (**b**) spodumene-quartz middlings, and (**c**) complex particles from the − 600/+ 300 μm

4.2.6 Theoretical Grade - Recovery Curves

A more functional method presenting the liberation is the mineralogically limiting grade-recovery curves. They are based on the calculated mass of spodumene and the total mass in each liberation category. Thus, the highest grade (> 80%, e.g., spodumene) is contained in the > 80% liberated spodumene particles. Then, the next category (60 to 80% liberation) is added, and the combined grade is calculated. This is repeated until all spodumene is accounted for.

The Li grade as a function of spodumene recovery curves by size fraction and calculated head is shown in Fig. 13. The best grades and recoveries are projected for the fine fraction and the lowest for the coarsest fraction. For example, Li grades of 3.2 to 3.7% for spodumene recovery of 99.5 to 85%, respectively, are expected for the head sample. These

calculates are based on the liberation of the spodumene particles, and it is assumed a perfect separation regardless of grain size. For example, for the − 600/+ 300 μm fraction, the first few particles to be recovered are well-liberated spodumene that will yield low recovery at a high grade of 3.6 Li. As flotation continues, the additional spodumene is recovered as middling particles with gangue minerals which will increase recovery but decrease the grade. Mineralogically limited grade-recovery analyses provide an indication of the theoretical maximum achievable elemental or mineral grade by recovery, based on individual particle liberation and grade. These results do not reflect any other recovery factors that could occur in the actual metallurgical process.

The Li grade as a function of spodumene recovery by size class is displayed in Fig. 14. The calculations indicate that the finest grain size spodumene will yield the highest grades and

Fig. 11 Spodumene exposure by size class for the size fractions and calculated for the head sample

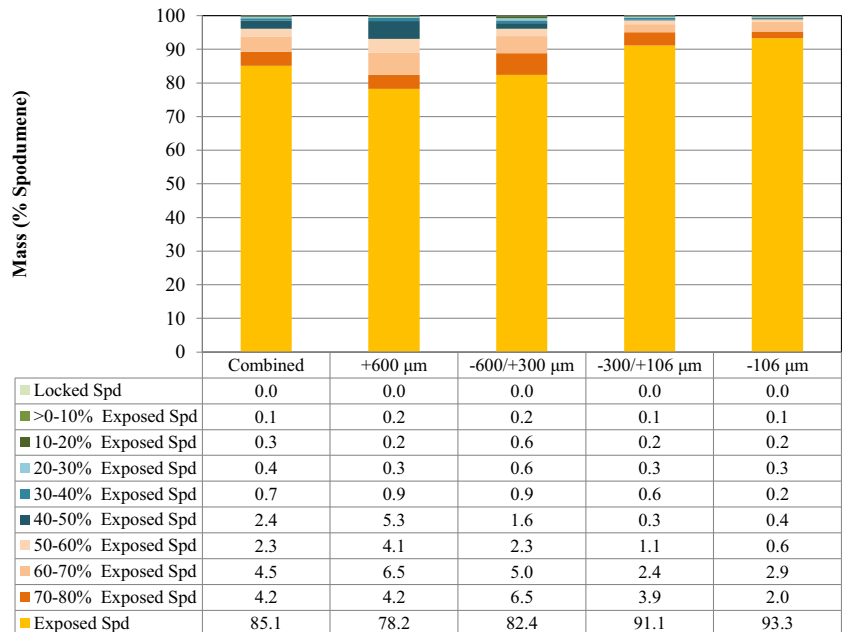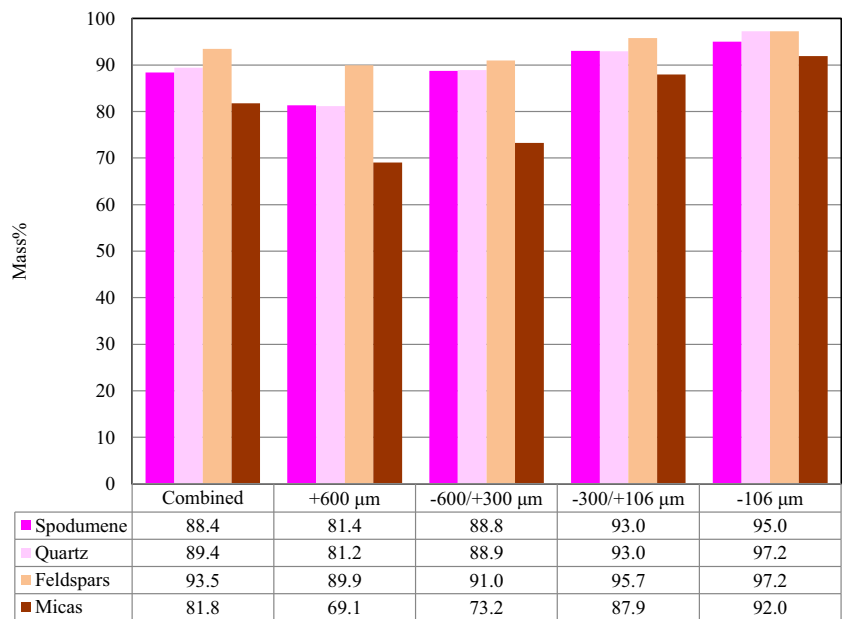|	Combined	+600 μm	-600/+300 μm	-300/+106 μm	-106 μm
Locked Spd	0.0	0.0	0.0	0.0	0.0
>0-10% Exposed Spd	0.1	0.2	0.2	0.1	0.1
10-20% Exposed Spd	0.3	0.2	0.6	0.2	0.2
20-30% Exposed Spd	0.4	0.3	0.6	0.3	0.3
30-40% Exposed Spd	0.7	0.9	0.9	0.6	0.2
40-50% Exposed Spd	2.4	5.3	1.6	0.3	0.4
50-60% Exposed Spd	2.3	4.1	2.3	1.1	0.6
60-70% Exposed Spd	4.5	6.5	5.0	2.4	2.9
70-80% Exposed Spd	4.2	4.2	6.5	3.9	2.0
Exposed Spd	85.1	78.2	82.4	91.1	93.3

Fig. 12 Liberation of spodumene, quartz, feldspars, and micas (mass%) by size fraction and calculated for the head

	Combined	+600 μm	-600/+300 μm	-300/+106 μm	-106 μm
Spodumene	88.4	81.4	88.8	93.0	95.0
Quartz	89.4	81.2	88.9	93.0	97.2
Feldspars	93.5	89.9	91.0	95.7	97.2
Micas	81.8	69.1	73.2	87.9	92.0

recoveries because they reflect their higher liberation. Thus, well-liberated particles in the range of 400–500 μm will yield very good grades at 3.6% Li with about 87% recovery. However, spodumene also occurs as middling particles in this class. Therefore, if the middlings are recovered then they will increase the spodumene recovery but will decrease the Li grade in the concentrate.

4.3 Mineral Chemistry by EPMA and LA-ICP-MS and Elemental Deportment

The chemistry of minerals is critical for the downstream applications. Elements such as Li, Cs, Rb, Ga, and Fe can vary widely in spodumene (e.g., [10]) but also micas and feldspars. Therefore, the Li and Fe concentrations in spodumene will affect the final Li grade of the concentrate, and its end use (i.e., ceramic or chemical grade, [6]). The chemical analyses of the minerals were conducted with both EPM and LA-ICP-

MS. Spodumene averages 3.7% Li, 6801 ppm Fe, 604 ppm Mn, and 131 ppm Ga (Table 6). The Li concentration is near the theoretical value [21] and suggests no lithium deficiency. However, a pure spodumene concentrate would have about 6801 ppm (or 0.68%) iron since the elemental impurities are part of the crystal structure of the mineral and cannot be physically removed. Any excess iron in the concentrate would be derived from other minerals (e.g., micas, amphibole).

Micas average 2196 ppm lithium and 6544 ppm rubidium 6544, 373 ppm Nb, 711 ppm Cs, 57 ppm Ta, and 270 ppm Ga (Table 7). Micas fall in between polylithionite and zinnwaldite solid solution field. The average lithium concentration in tourmaline is 1001 ppm, and 185 ppm Ga. K-feldspars average 5771 ppm Rb and 528 ppm Cs, and 115 ppm Li. Two Fe-Mn phosphate grains, possibly sicklerite $Li(Mn,Fe)PO_4$, contain 1.5 to 9.0% lithium.

Subsequently, the distribution of lithium, rubidium, and cesium is calculated based on the mineral mass as

Fig. 13 Li grade as a function of spodumene recovery by size fraction and calculate head (lower 90% exposure and upper 40–50% exposure)
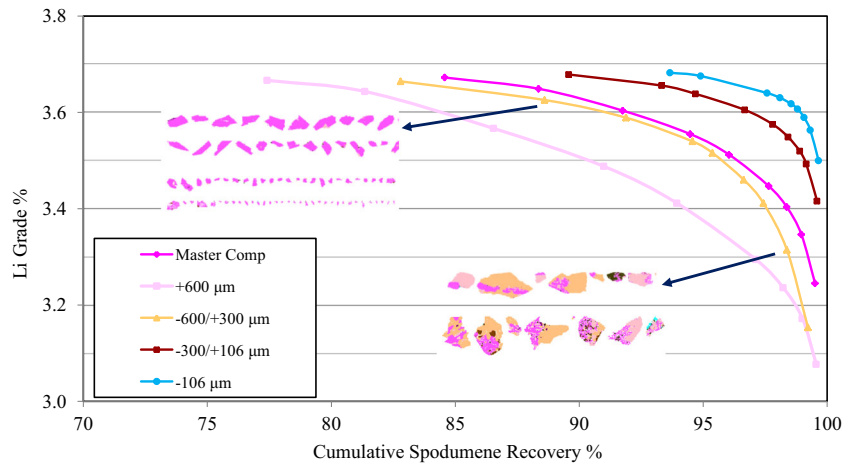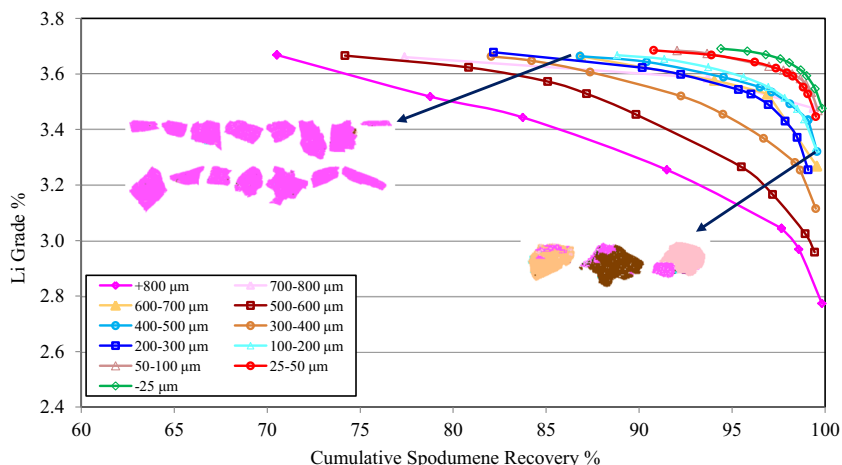
Fig. 14 Li grade as a function of spodumene recovery by size classes (upper < 30% exposure and 400–500 μm and lower > 90% exposure for 400–500 μm)

4.4 Heavy Liquid Separation Testwork

determined with the QEMSCAN, and the average composition of each mineral of interest. Spodumene accounts for 95.8%, Li-phosphates for 0.5%, tourmaline for 0.7%, and micas for 2.1% of the total lithium in the sample (Fig. 15). The low grade of micas and phosphates and the low Li concentrations favor a spodumene concentrate, and minimum losses due to Li hosted by other minerals. K-feldspars host 81% and micas 19% of the total Rb in the sample. Micas carry most of the Cs (68%), followed by K-feldspars (28%) and spodumene (< 4%).

A heavy liquid separation (HLS) test was conducted to assess the amenability of the sample to dense media separation (DMS) for the beneficiation of spodumene. The − 6.4 mm/+ 600 μm fraction was submitted for the HLS test, in which eight heavy liquid-specific gravity cut-points (3.10, 3.00, 2.95, 2.90, 2.80, 2.70, 2.65 g/cm^3) were evaluated. These heavy liquids were made by proportionally mixing methylene iodide with density of 3.32 g/cm^3 and acetone with density of 0.78 g/cm^3 to achieve the target density.

Table 6 Detection limits (LOD), and minimum (Min), maximum (Max), and average (Ave) values from the EPM and LA-ICP-MS analyses of spodumene

$N = 19$ EPMA, wt%	LOD	Min	Max	Ave	LA-ICP-MS, ppm	LOD	Min	Max	Ave
Na2O	0.018	0.04	0.20	0.12	Li	2.0	31,630	37,940	36,572
MgO	0.018	0.00	0.02	0.01	Li%		3.16	3.79	3.66
Al2O3	0.017	26.16	27.27	26.83	Na	17	448	1380	986
SiO2	0.022	61.29	64.79	63.35	Mg	1	2	4080	305
P2O5	0.034	0.00	0.02	0.00	P	31	1	90	32
K2O	0.019	0.00	0.02	0.00	K	10	0	1373	165
CaO	0.021	0.00	0.09	0.03	Ca	152	1	311	87
TiO2	0.066	0.00	0.05	0.01	Sc	1	2	31	15
MnO	0.060	0.02	0.11	0.06	Ti	2	10	78	33
FeO	0.065	0.41	1.44	0.84	Mn	3	197	1280	604
Rb2O	0.032	0.01	0.05	0.03	Fe	5	2368	11,610	6801
Cs2O	0.038	0.00	0.00	0.00	Zn	1	3	44	13
BaO	0.232	0.00	0.10	0.04	Ga	1	83	177	131
F	0.039	0.00	0.00	0.00					
Cl	0.014	0.00	0.01	0.00					
Total		89.01	92.49	91.32					

Table 7 Detection limits (LOD), and minimum (Min), maximum (Max), and average (Ave) values EPM and LA-ICP-MS analyses of micas

$N = 19$ EPMA, wt%	LOD	Min	Max	Ave	LA-ICP-MS, ppm	LOD	Min	Max	Ave
Na2O	0.018	0.23	0.45	0.34	Li	2	930	4010	2196
MgO	0.018	0.10	0.16	0.13	Li%		0.09	0.40	0.22
Al2O3	0.017	31.73	34.85	33.49	Na	17	1633	3610	2618
SiO2	0.022	42.41	45.38	44.25	Mg	1	315	1169	714
P2O5	0.034	0.00	0.04	0.01	Sc	1	4	49	29
K2O	0.019	9.70	10.06	9.90	Ti	2	159	730	476
CaO	0.021	0.00	0.03	0.01	Mn	3	305	1136	703
TiO2	0.066	0.05	0.17	0.10	Fe	5	17,180	41,450	25,513
MnO	0.060	0.01	0.16	0.09	Zn	1	110	987	569
FeO	0.065	2.75	5.46	3.90	Ga	1	188	315	270
Rb2O	0.032	0.52	0.75	0.60	Rb	1	4925	8114	6544
Cs2O	0.038	0.00	0.22	0.06	Nb	1	101	525	373
BaO	0.232	0.00	0.14	0.04	Cs	1	246	2324	711
F	0.039	0.15	1.03	0.57	Ta	1	29	92	57
Cl	0.014	0.00	0.03	0.01					
Total		91.68	94.80	93.26					

Generally speaking, in each pass of a heavy liquid test, the material is initially added to the heavy liquid in the separation vessel, stirred vigorously, and then progressively less vigorously. The stirring is stopped when the sinking material feels heavy on the mixing rod. A few minutes are then allowed to achieve perfect separation, which is determined to be once the liquid between the floating and sinking portion is free from particles. The float material is then removed from the surface of the heavy liquid, and the sink material is removed from the separation vessel by opening the separation valve. In this case,

considering that the sample was fairly coarse, − 6.4 mm/+ 600 μm, the separation in the heavy liquid was fairly fast.

In the HLS test, the first pass was conducted using a heavy liquid with the highest specific gravity (3.10), and each subsequent pass was conducted using a heavy liquid with lower specific gravity. The float product from each pass served as the feed to the subsequent pass. The results of the HLS test (Table 8) clearly indicate that the spodumene concentrate generated in this test (combined sink product with SG cut-point of 3.00) had relatively low grade, 5.42% Li$_2$O, which is less than

Fig. 15 Lithium, Cs, and Rb deportment calculated for the head

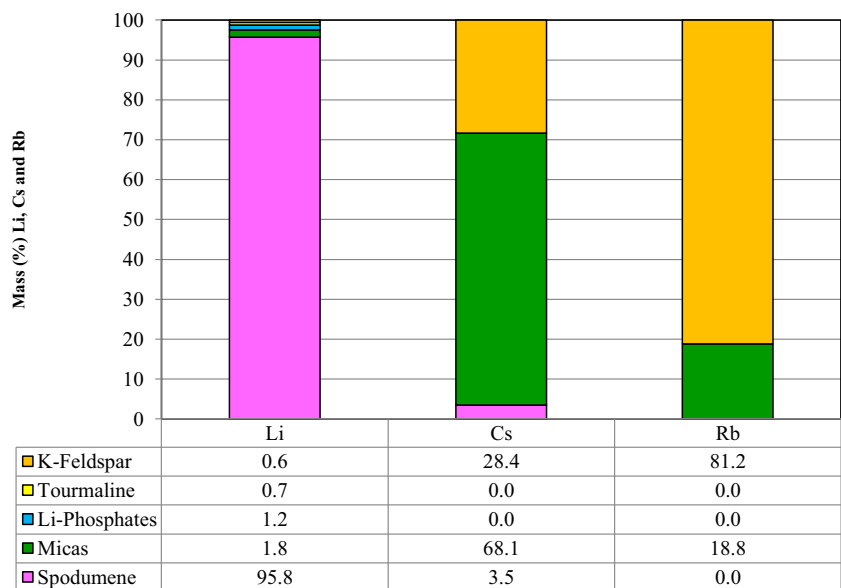|	Li	Cs	Rb
K-Feldspar	0.6	28.4	81.2
Tourmaline	0.7	0.0	0.0
Li-Phosphates	1.2	0.0	0.0
Micas	1.8	68.1	18.8
Spodumene	95.8	3.5	0.0

Table 8 HLS test results including the SG (specific gravity), weight (g and % distribution), assays of major elements, and their distribution

Global mass balance

HLS products	HL SG	Weight		Assays (%)										Distribution (%)								
	g/cm³	g	%	Li	Li₂O	SiO₂	Al₂O₃	Fe₂O₃	MgO	CaO	Na₂O	K₂O	P₂O₅	Li	SiO2	Al₂O₃	Fe₂O₃	MgO	CaO	Na₂O	K₂O	P₂O₅
HLS sink 3.10	3.10	215	2.2	2.45	5.28	57.16	25.86	5.00	0.69	0.67	0.49	0.16	0.24	14.4	1.7	3.5	10.7	7.0	2.8	0.3	0.1	2.1
HLS sink 3.00	3.00	345	3.5	2.56	5.51	61.47	25.49	2.87	0.40	0.61	0.41	0.35	0.23	24.1	3.0	5.6	9.8	6.6	4.1	0.4	0.3	3.3
HLS sink 2.95	2.95	245	2.5	2.40	5.15	63.38	23.90	2.42	0.46	0.74	0.48	0.46	0.29	16.0	2.2	3.7	5.9	5.4	3.5	0.3	0.3	3.0
HLS sink 2.90	2.90	123	1.2	1.73	3.72	65.44	20.94	2.60	0.59	1.01	0.91	1.15	0.42	5.8	1.1	1.6	3.2	3.4	2.4	0.3	0.4	2.1
HLS sink 2.80	2.80	491	4.9	0.47	1.01	60.90	23.20	2.77	0.51	0.76	1.19	4.34	0.30	6.3	4.2	7.2	13.5	11.9	7.3	1.7	5.6	6.1
HLS sink 2.70	2.70	651	6.5	0.35	0.75	71.80	16.60	1.68	0.31	0.85	2.51	2.64	0.40	6.2	6.5	6.8	10.9	9.6	10.8	4.8	4.5	10.7
HLS sink 2.65	2.65	713	7.1	0.12	0.26	80.40	10.90	0.74	0.16	0.57	3.16	1.60	0.27	2.3	8.0	4.9	5.2	5.4	7.9	6.6	3.0	7.9
HLS float 2.65	2.65	5299	53.1	0.04	0.09	73.90	14.30	0.21	0.10	0.34	4.37	4.96	0.19	6.2	54.6	47.9	11.0	25.3	35.2	67.8	68.8	41.4
−600 µm	-	1892	19.0	0.36	0.77	71.30	15.70	1.59	0.28	0.70	3.21	3.46	0.30	18.6	18.8	18.8	29.8	25.3	25.9	17.8	17.1	23.3
Feed (Calc.)		9974	100	0.37	0.79	71.94	15.86	1.01	0.21	0.51	3.43	3.83	0.24	100	100	100	100	100	100	100	100	100
Feed (Dir.)				0.44	0.95	71.90	15.90	1.06	0.20	0.51	3.48	3.91	0.22									

the target 6% Li₂O. Furthermore, the Fe₂O₃ content was considered high at 3.7% in this combined product. This low-grade concentrate is due to the large amount of iron silicate minerals (possibly amphiboles or tourmaline) reporting to the spodumene concentrate.

Therefore, magnetic separation was conducted on the selected HLS products to reject the Fe carriers. A dry magnetic belt separator operating at a magnetic intensity of about 8000 G was used to reject iron silicate minerals from the heavy liquid concentrates.

The results (Table 9 and Fig. 16) are significantly improved after performing magnetic separation on the selected HLS products (sink products with SG cut-points of 3.10, 3.00, 2.95, and 2.90 g/cm³). Iron silicate minerals were rejected by magnetic separation to achieve a concentrate grade of 6.04% Li₂O (in the combined sink product with SG cut-point of 3.00) with a recovery of 38.1%. This indicates that the ore contains a fairly large amount of spodumene grains (at least about 38%) which can be recovered by dense media separation (DMS). A summary of the HLS test results with the magnetic separation is shown in Table 10. It can be concluded that 33.8% of the mass reported to the combined HLS middling and undersize fraction (flotation circuit feed) with the grade of 1.23% Li₂O (which is higher than the head grade) and with lithium recovery of 52.7%. Approximately, 60.3% of the mass reported to the tailing with lithium losses of 8.6%; and 0.7% of lithium was lost in the magnetic concentrate with the mass pull of 1.0%. The mass yield to the sink product with SG cut of 3.00 g/cm³ was 5%.

Fe silicates in this sample have a density in the range of (2.9 to 3.1 g/cm³), which interferes with the separation of spodumene from the ore. As a result of the deportment of iron silicate minerals to the HLS spodumene concentrate, the concentrate lithium grade becomes lower than expected, with high iron content. Thus, pre-rejection of these gangue minerals (with ore sorting or magnetic separation) is expected to be quite beneficial.

Recovery of spodumene by dense media separation (DMS) is a function of spodumene grain size. Lithium ores, with high potential for beneficiation by DMS, are expected to produce a good portion of spodumene concentrate in the DMS operation. In the absence of a feasibility study, it is difficult to conclude the minimum amount of DMS spodumene concentrate required to financially justify DMS operations. However, it is assumed that lithium recovery to DMS concentrate of the target grade should be at least in the range of 30 to 50%. In this study, the results indicate that there is a potential to recover 38% of the feed lithium in the DMS spodumene concentrate at a concentrate grade of 6.04% Li₂O. If lower concentrate grade, 5.8% Li₂O, is acceptable, about 54% of the feed lithium can be recovered in the DMS operation. The current results show that the investigated ore sample is highly amenable to spodumene beneficiation by DMS operation.

Table 9 HLS separation test results after magnetic separation including the SG (specific gravity), weight (g and % distribution), assays of major elements, and their distribution

	HL SG	Weight		Assays (%)										Distribution (%)								
	g/cm³	g	%	Li	Li₂O	SiO₂	Al₂O₃	Fe₂O₃	MgO	CaO	Na₂O	K₂O	P₂O₅	Li	SiO2	Al₂O₃	Fe₂O₃	MgO	CaO	Na₂O	K₂O	P₂O₅
Global mass balance																						
HLS products																						
HLS sink 3.10 non-mag	3.10	181	1.8	2.86	6.15	61.0	25.1	3.01	0.62	0.44	0.25	0.17	0.15	14.2	1.5	2.9	5.4	5.4	1.6	0.1	0.1	1.1
HLS sink 3.00 non-mag	3.00	316	3.2	2.78	5.98	63.5	25.4	1.79	0.26	0.35	0.29	0.34	0.21	24.0	2.8	5.1	5.6	3.9	2.2	0.3	0.3	2.7
HLS sink 2.95 non-mag	2.95	234	2.3	2.50	5.38	64.4	23.9	1.89	0.37	0.57	0.42	0.43	0.26	15.9	2.1	3.5	4.4	4.1	2.6	0.3	0.3	2.5
HLS sink 2.90 non-mag	2.90	107	1.1	1.93	4.15	67.6	20.8	1.71	0.35	0.68	0.83	0.85	0.39	5.6	1.0	1.4	1.8	1.8	1.4	0.3	0.2	1.7
HLS sink 2.80	2.80	491	4.9	0.47	1.01	60.9	23.2	2.77	0.51	0.76	1.19	4.34	0.30	6.3	4.2	7.2	13.5	11.9	7.3	1.7	5.6	6.1
HLS sink 2.70	2.70	651	6.5	0.35	0.75	71.8	16.6	1.68	0.31	0.85	2.51	2.64	0.40	6.2	6.5	6.8	10.9	9.6	10.8	4.8	4.5	10.7
HLS sink 2.65	2.65	713	7.1	0.12	0.26	80.4	10.9	0.74	0.16	0.57	3.16	1.60	0.27	2.3	8.0	4.9	5.2	5.4	7.9	6.6	3.0	7.9
HLS float 2.65	2.65	5299	53.1	0.04	0.09	73.9	14.3	0.21	0.1	0.34	4.37	5.0	0.19	6.2	54.6	47.9	11.0	25.3	35.2	67.8	68.8	41.4
− 600 µm	-	1892	19.0	0.36	0.77	71.3	15.7	1.59	0.28	0.7	3.21	3.46	0.30	18.6	18.8	18.8	29.8	25.3	25.9	17.8	17.1	23.3
HLS sink 3.10 mag	-	33.2	0.3	0.24	0.52	36.2	30.0	15.9	1.05	1.92	1.8	0.12	0.75	0.2	0.2	0.6	5.2	1.7	1.2	0.2	0.0	1.0
HLS sink 3.00 mag	-	29.2	0.3	0.22	0.47	39.5	26.5	14.5	1.96	3.48	1.71	0.47	0.49	0.2	0.2	0.5	4.2	2.7	2.0	0.1	0.0	0.6
HLS sink 2.95 mag	-	11.6	0.1	0.30	0.65	42.9	23.9	13.1	2.25	4.12	1.73	0.99	0.98	0.1	0.1	0.2	1.5	1.2	0.9	0.1	0.0	0.5
HLS sink 2.90 mag	-	15.9	0.2	0.39	0.84	50.9	21.9	8.62	2.18	3.26	1.43	3.16	0.63	0.2	0.1	0.2	1.4	1.7	1.0	0.1	0.1	0.4
Feed (Calc.)	-	9974	100	0.37	0.79	71.9	15.9	1.01	0.21	0.51	3.43	3.83	0.24	100	100	100	100	100	100	100	100	100
Feed (Dir.)				0.44	0.95	71.9	15.9	1.06	0.20	0.51	3.48	3.91	0.22									
Combined sink results																						
Combined HLS products																						
HLS sink 3.10	3.10	181	1.8	2.86	6.15	61.0	25.1	3.01	0.62	0.44	0.25	0.17	0.15	14.2	1.5	2.9	5.4	5.4	1.6	0.1	0.1	1.1
HLS sink 3.00	3.00	497	5.0	2.81	6.04	62.6	25.3	2.23	0.39	0.38	0.28	0.28	0.19	38.1	4.3	7.9	11.0	9.3	3.7	0.4	0.4	3.8
HLS sink 2.95	2.95	731	7.3	2.71	5.83	63.2	24.8	2.12	0.38	0.44	0.32	0.33	0.21	54.1	6.4	11.5	15.4	13.4	6.3	0.7	0.6	6.3
HLS sink 2.90	2.90	838	8.4	2.61	5.61	63.7	24.3	2.07	0.38	0.47	0.39	0.39	0.23	59.7	7.4	12.9	17.2	15.2	7.7	0.9	0.9	8.1
HLS sink 2.80	2.80	1329	13.3	1.82	3.91	62.7	23.9	2.33	0.43	0.58	0.68	1.85	0.26	66.0	11.6	20.1	30.7	27.1	15.0	2.7	6.4	14.1
HLS sink 2.70	2.70	1980	19.9	1.34	2.87	65.7	21.5	2.12	0.39	0.67	1.28	2.11	0.30	72.2	18.1	26.9	41.6	36.8	25.8	7.4	10.9	24.8
HLS sink 2.65	2.65	2693	27.0	1.01	2.18	69.6	18.7	1.75	0.33	0.64	1.78	1.98	0.30	74.5	26.1	31.8	46.8	42.2	33.8	14.0	13.9	32.8
Combined float results																						
Combined HLS products																						
HLS float 3.10	3.10	7811	78.3	0.31	0.67	72.7	15.6	0.68	0.17	0.44	3.57	4.04	0.23	66.6	79.1	76.8	52.4	62.1	67.4	81.7	82.6	73.0
HLS float 3.00	3.00	7495	75.1	0.21	0.45	73.1	15.2	0.63	0.16	0.45	3.71	4.20	0.23	42.6	76.4	71.8	46.8	58.2	65.2	81.4	82.3	70.3
HLS float 2.95	2.95	7261	72.8	0.13	0.29	73.4	14.9	0.59	0.16	0.44	3.82	4.32	0.23	26.7	74.3	68.2	42.4	54.1	62.6	81.1	82.0	67.8
HLS float 2.90	2.90	7154	71.7	0.11	0.23	73.5	14.8	0.57	0.15	0.44	3.86	4.37	0.22	21.1	73.2	66.8	40.6	52.3	61.2	80.8	81.8	66.1
HLS float 2.80	2.80	6663	66.8	0.08	0.17	74.4	14.2	0.41	0.13	0.41	4.06	4.37	0.22	14.8	69.1	59.6	27.1	40.3	53.9	79.1	76.2	60.0
HLS float 2.70	2.70	6012	60.3	0.05	0.11	74.7	13.9	0.27	0.11	0.37	4.23	4.56	0.20	8.6	62.6	52.8	16.3	30.7	43.1	74.3	71.7	49.3
HLS float 2.65	2.65	5299	53.1	0.04	0.09	73.9	14.3	0.21	0.10	0.34	4.37	4.96	0.19	6.2	54.6	47.9	11.0	25.3	35.2	67.8	68.8	41.4

Table 10 Summary of the HLS test results including the SG (specific gravity), weight (g and % distribution), assays of major elements, and their distribution

Combined Floats Results

| Combined HLS products	Weight		Assays (%)										Distribution (%)								
	g	%	Li	Li2O	SiO2	Al2O3	Fe2O3	MgO	CaO	Na2O	K2O	P2O5	Li	SiO2	Al2O3	Fe2O3	MgO	CaO	Na2O	K2O	P2O5
HLS Conc (sink 3.00 g/cm³)	497	5.0	2.81	6.04	62.6	25.3	2.23	0.39	0.38	0.28	0.28	0.19	38.1	4.3	7.9	11.0	9.3	3.7	0.4	0.4	3.8
HLS middlings & – 600 μm	3375	33.8	0.57	1.23	69.3	17.7	1.80	0.33	0.73	2.51	3.14	0.32	52.7	32.6	37.7	60.4	52.7	48.0	24.8	27.7	44.3
Silicate tail (float 2.70 g/cm³)	6012	60.3	0.05	0.11	74.7	13.9	0.27	0.11	0.37	4.23	4.56	0.20	8.6	62.6	52.8	16.3	30.7	43.1	74.3	71.7	49.3
Mag Conc.	89.9	0.9	0.27	0.58	40.7	26.6	13.80	1.70	2.95	1.70	0.88	0.67	0.7	0.5	1.5	12.3	7.3	5.2	0.4	0.2	2.5
Feed (Calc.)	9974	100	0.37	0.79	71.9	15.9	1.01	0.21	0.51	3.43	3.83	0.24	100	100	100	100	100	100	100	100	100

5 Discussion

Quantitative mineralogy for any project is critical because it can quantify mineralogical parameters applicable to mineral processing such as grain size, liberation, and association of the minerals of interest and gangue. Spodumene is well liberated at 88% in the Master Comp and increases from 81 in the + 600 μm to 95% in the 106 μm. Therefore, a decision will have to be made based on the economics of the project such as grinding energy, and grade and recovery trade off.

The gangue minerals are also well liberated at a P_{80} of 600 μm. Therefore, theoretically, they could be removed to further increase the Li grade of a spodumene concentrate. Some spodumene middling particles with gangue would be inevitably recovered and will result in mainly Na, K impurities given the inherent textural relations. However, additional selective and finer grinding would further liberate the spodumene as shown by the liberation profile of the mineral. Selective grinding might also increase the amount of spodumene with {110} that appear to respond better to flotation. The aspect ratio as estimated with the QEMSCAN could be a potential tool to estimate the {110} planes of the spodumene. The mineralogical results indicate that grades between 3.1 and 3.7% are achievable for the head sample at a P_{80} of 600 μm. A pure spodumene concentrate would contain about 0.68% Fe.

Mineral chemistry is important to determine the Li and trace elements in the spodumene but also in other associated minerals. Li in spodumene might vary among deposits due to geological effects (e.g., alteration). Micas contain minor Li which will not affect the overall Li distribution in the sample. The pegmatites contain relatively low grades of Ta, but considerable Cs and Rb that are carried by feldspars and micas. These are also well liberated and could be considered by-products during flotation. Cs and Rb might be by-products from the Li but their economic feasibility has to be further evaluated. Furthermore, Zhu et al. [22] showed that the natural spodumene crystals have lattice defects, including isomorphous substitution of Fe, Mn, and Cr. Such substitutions affect surface features, such as hydrophobicity of minerals and collector adsorption on mineral surfaces. Micro-flotation experiments, FTIR analysis, and contact angle results showed that higher Fe contents favored for the oleate adsorption on spodumene surface. Therefore, proper analytical methods and accurate determination of elemental substitutions in the spodumene lattice can be further evaluated in flotation response of the mineral.

The mineralogy of the spodumene concentrate and association of spodumene with other minerals is important in roasting. A major transformation of α-spodumene to β-spodumene occurs around 1000 °C during roasting. The behavior of spodumene at increased temperatures can depend on several factors, with the predominant factor being the

Fig. 16 Grade/recovery and mass pull as a function of HLS density
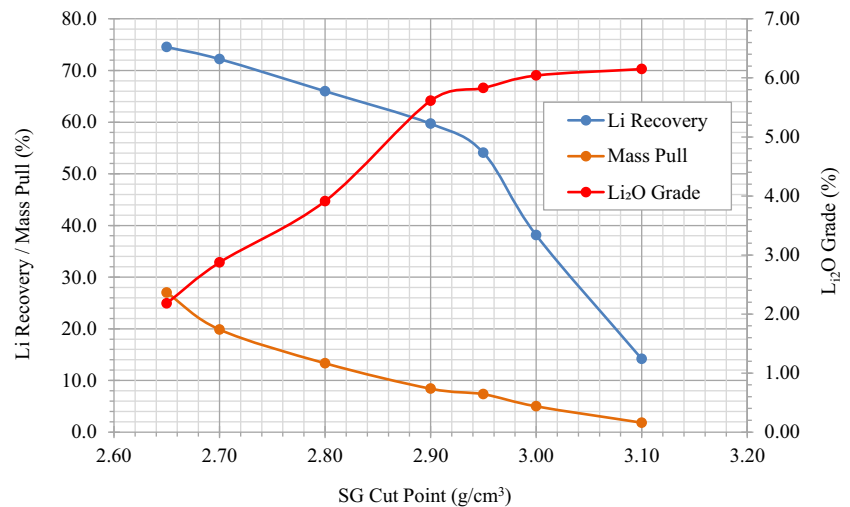
interlocked impurities. Higher amounts of impurities cause lower conversion temperatures ([23, 24] and references therein).

Beneficiation of spodumene typically includes heavy media separation, magnetic separation, and flotation followed by pyrometallurgical and hydrometallurgical processes to extract the Li (i.e., $LiCO_3$) (e.g., [6, 23] and references therein). The results from the HLS indicate that a large mass of the gangue minerals could be rejected to the tailings at coarse sizes (-6.4 mm) with low lithium losses. HLS and magnetic separation indicate that it is possible to achieve a spodumene concentrate with 2.81% Li (or 6.04% Li_2O) grade and spodumene recovery of about 38%. Magnetic separation was successful in rejecting iron silicate minerals which are mainly associated with waste material and derived from the hanging wall, a separate zone from pegmatite. Thus, the expected liberation for the waste material is good even at the coarse crushing size. As a result, ore sorting has the potential to reject waste materials with a relatively coarse crushing size of $+12$ mm. Magnetic separation on the other hand can be used on the finer fraction, -6.4 mm, to reject silicate gangue minerals ahead of the DMS operation and prevent the deportment of these waste materials to the DMS spodumene concentrate.

flotation can be conducted at relatively coarse particle size to recover the spodumene. Liberation of gangue minerals including quartz (89%), Na- and K-feldspars (94%), and micas (82%) is very good. These can theoretically be rejected. Preliminary testwork, HLS and combined with magnetite separation, tests indicate that it is possible to produce a high-grade (close to 6% Li_2O) lithium concentrate after the rejection of iron silicate minerals. Thus, most of the spodumene should be amenable to recovery by HLS and/or flotation. The mineralogical characteristics of the pegmatite favor the economic potential of the project. However, additional metallurgical testwork should be further conducted to evaluate the DMS and flotation recovery of spodumene.

Compliance with Ethical Standards

Conflict of Interest The authors declare that they have no conflict of interest.

6 Conclusions

Automated mineralogy, coupled with geochemical analyses and mineral chemistry, provide valuable quantitative data that can be used to guide the test work and explain recoveries and potential losses. Spodumene is the primary lithium mineral in the Zoro Pegmatite and accounts for 96% of the total lithium. Lithium losses due to other than spodumene host minerals will be minimal and favor the project. Furthermore, liberation of spodumene is 88% for the calculated head for a P_{80} of 600 μm. Therefore,

References

1. Jaskula BW (2014) 2014 minerals yearbook. Lithium. U.S.Geological Survey, U.S. Department of the Interior. http://minerals.usgs.gov/minerals/pubs/commodity/lithium/myb1-2014-lithi.pdf

2. Goonan TG (2012) Lithium use in batteries. U.S. Geological Survey, US Department of the Interior http://pubs.usgs.gov/circ/1371/pdf/circ1371_508.pdf

3. Bulatovic SM (2014) Beneficiation of lithium ores. In S. M. Bulatovic, Handbook of Flotation Reagents: Chemistry, Theory and Practice – Volume 3: Flotation of Industrial Minerals (pp. 41–56). Elsevier B.V

4. Ober JA (1994) 1994 minerals yearbook. Lithium. U.S. Geological Survey, U.S. Department of the Interior. http://minerals.usgs.gov/minerals/pubs/commodity/lithium/450494.pdf

5. Gasalla HJ, Aglietti EF, Lopez JMP, Pereira E (1987) Changes in physicochemical properties of α-spodumene by mechanochemical treatment. Mater Chem Phys 17:379–389

6. Gibson C, Aghamirian M, Grammatikopoulos T (2017) The beneficiation of lithium minerals from hard rock deposits. Min Eng 69:8

7. Heinrich EW, Salotti CA, Giardini AA (1978) Hydrogen- mineral reactions and their application to the removal of iron from spodumene. Energy 3:273–279

8. Clarke GM (2013) Lithium-ion batteries: raw material considerations. Chem Eng Prog 109:44–52

9. Grammatikopoulos TA, Pearse G, Gelcich S, Gunning C (2009) Quantitative characterization of spodumene ore by automated mineralogy from the Moblan rare metals pegmatite deposit, Quebec, Canada. In: Proceedings of the 48th Annual Conference of Metallurgists of CIM (MetSoc), pp. 65–76

10. Aylmore MG, Merigot K, Rickard WDA, Evans NJ, McDonald BJ, Catovic E, Spitalny P (2018) Assessment of a spodumene ore by advanced analytical and mass spectrometry techniques to determine its amenability to processing for the extraction of lithium. Miner Eng 119:137–148

11. Vizcarra TG, Harmer SL, Wightman EM, Johnson NW, Manlapig EV (2011) The influence of particle shape properties and associated surface chemistry on the flotation kinetics of chalcopyrite. Miner Eng 24:807–816

12. Jameson GJ (2012) The effect of surface liberation and particle size on flotation rate constants. Miner Eng 36–38:132–137

13. Xu L, Hu Y, Wu H, Tian J, Liu J, Gao Z, Wang L (2016) Purif Technol 169:33–42

14. Filippov L, Farrokhpay S, Lyo L, Filippova I (2019) Spodumene flotation mechanism. Minerals 9:372. https://doi.org/10.3390/min9060372

15. Beland C (2011) Geochemistry and geochronology of the Whabouchi pegmatite dykes as revealed through zircon. B.Sc., thesis, 99p

16. Sousa R, Ramos V, Guedes A, Botelho de Sousa A, Noronha F, Machado Leite M (2019) Flotation of lithium ores to obtain high-grade Li_2O concentrates. Are there any mineralogical limitations? Int J Min Mater Metall Eng (IJMMME) 5:7–18

17. Thomas RJ, Bühmann D, Bullen WD, Scogings AJ, De Bruin D (1994) Unusual spodumene pegmatites from the Late Kibaran of southern Natal, South Africa. Ore Geol Rev 9:161–182

18. London D (1984) Experimental phase equilibria in the system $LiAlSiO_4$-SiO_2-H_2O: a petrogenetic grid for lithium-rich pegmatites. Am Miner 69:995–1004

19. Selway JB, Breaks FW, Tindle AG (2005) A review of rare-element (Li-Cs-Ta) pegmatite exploration techniques for the Superior Province, Canada, and large worldwide tantalum deposits. Explor Min Geol 14(1–4):1–30

20. Tian J, Xu L, Wu H, Fang S, Deng W, Peng T, Sun W, Hu Y (2018) A novel approach for flotation recovery of spodumene, mica and feldspar from a lithium pegmatite ore. J Clean Prod 174:625–633

21. Deer WA, Howie RA, Zussman J (1978) Rock-forming minerals, 2A. Single-Chain Silicates, Longman

22. Zhu G, Cao Y, Wang Y, Wang X, Miller JD, Lu D, Zheng X (2020) Surface chemistry features of spodumene with isomorphous substitution. Miner Eng 146:106139. https://doi.org/10.1016/j.mineng.2019.106139

23. Salakjani NK, Singh P, Nikoloski AN (2019) Production of Lithium – a literature review part 1: pretreatment of Spodumene. Miner Process Extr Metall Rev 41:335–348. https://doi.org/10.1080/08827508.2019.1643343

24. Tian Q, Chen B, Chen Y, Ma I, Shi X (2011) Roasting and leaching behaviour of spodumene in sulfuric acid process. Chin J Rare Metals 35:118–123